SOURCE: Jerome P. Lynch, " Damage Characterization of the IASC-ASCE Structural Health Monitoring Benchmark Structure by Transfer Function Pole Migration, " *Proceedings of the 2005 ASCE Structures Congress*, New York, NY, April 20-23, 2005. 2005.

Damage Characterization of the IASC-ASCE Structural Health Monitoring Benchmark Structure by Transfer Function Pole Migration

J. P. Lynch

University of Michigan, Department of Civil and Environmental Engineering, 2328 G. G. Brown Building, Ann Arbor, MI 48109-2125; Ph (734) 615-5290; email: jerlynch@umich.edu (http://www.engin.umich.edu/dept/cee/)

Abstract

In this paper, a novel approach to the characterization of structural damage in civil structures is presented. Structural damage often results in subtle changes to structural stiffness and damping properties that are manifested by changes in the location of transfer function characteristic equation roots (poles) upon the complex plane. Using structural response time-history data collected from an instrumented structure, transfer function poles can be estimated using traditional system identification methods. Comparing the location of poles corresponding to the structure in an unknown structural state to those of the undamaged structure, damage can be accurately identified. The IASC-ASCE structural health monitoring benchmark structure is used in this study to illustrate the merits of the transfer function pole migration approach to damage detection in civil structures.

Introduction

Civil infrastructures are complex engineered systems that are designed to carry massive loads while ensuring the safety of system users. These complex structures can experience deterioration and damage as a result of excessive loading commonly associated with seismic, blast and live loads. In recent years, the structural engineering field has begun to undertake research aimed at advancing sensing technologies so that low-cost structural monitoring systems can be created. Microelectromechanical system (MEMS) sensors, wireless telemetry, fiber optic strain sensors, among others, are all fruits of these efforts. With new structural sensing technologies enjoying lower costs, expanded functionality, and enhanced sensitivity, the installation of structural monitoring systems in civil structure is more compelling than ever before. The data collected by structural monitoring systems can be used to characterize properties of the structural system and to potentially identify the onset of structural damage. Since manual inspection of structural response data for signs of damage might not represent a desirable nor scalable solution, automated damage detection algorithms are needed. When these damage detection algorithms are embedded and autonomously executed by the structural monitoring system, the system is transformed into a structural health monitoring system. An immediate benefit of structural health monitoring systems is that they offer facility managers the opportunity to adopt condition-based maintenance strategies in lieu of today's schedule-based approaches.

Different damage detection algorithms have been proposed for a variety of structural systems including those for mechanical, aeronautical and civil structures (Doebling *et al.* 1996). The vast majority of these damage detection methods have originated under the assumption that only a small number of sensors are available for recording the dynamic response of the system. As such, the methods are primarily global-based damage detection methods that seek to correlate measurable changes in modal properties to structural damage. Particularly for civil structures, these approaches have been hampered by their sensitivity to a structure's environmental factors (e.g. temperature); thus, the onset of structural damage can be difficult to detect. However, in recent years, there has been a renewed interest in formulating new approaches to damage detection that are more robust in the face of environmental factors. In particular, new damage detection methods receiving recent attention all include the use of new analytical tools such as pattern recognition (Sohn and Farrar 2001), Bayesian system identification (Yuen, Au and Beck 2004) and active sensing impedance spectroscopy (Park, Cudney and Inman 2000). To validate and compare the performance of current and future damage detection methodologies, a powerful structural health monitoring benchmark study has been devised that offers an extensive data set collected from a full-scale laboratory structure tested under ambient and forced vibrations. Since the public release of the IASC-ASCE Task Group on Structural Health Monitoring's benchmark study, a number of researchers have tested the efficacy of their damage detection strategies on the data set (Johnson *et al.* 2004).

In this study, a novel damage detection approach is taken to analyze empirical response data corresponding to the IASC-ASCE benchmark structural health monitoring structure. Damage in civil structures is often accompanied by subtle changes in system stiffness and damping properties. Using input-output response data of the structure, complex-domain transfer functions that describe the undamaged structural system are first estimated. When the structure is in an unknown structural state (potentially damaged), transfer function characteristic equation roots are compared to those of the undamaged structure to identify if their location upon the complex plane has undergone a statistically significant migration. The approach presented is an extension of an analytical methodology recently proposed for detecting crack damage in structural plates excited and monitored using piezoelectric actuators and sensors (Lynch 2004).

Damage Induced Migration of Complex Domain Transfer Function Poles

Early damage detection methods principally employed changes in modal properties (namely, modal frequencies and mode shapes) to identify the occurrence of structural damage. Both properties of a dynamic system can be estimated by applying ordinary modal analysis to response data recorded from a vibrating structure. Modal frequencies and mode shapes are attractive parameters to investigate for damage because they are dependent upon the mass and stiffness properties of the structure. However, modal parameters have proven to be difficult damage indicators for civil structures because their estimation is often based on a poorly conditioned inverse problem. Alternatively, newer damage detection algorithms have suggested the value of using the estimated parameters of input-output and output-only system identification models for damage detection. Such approaches have proven successful when cast within a statistical framework offered by pattern classification theory. Examples of this approach include the use of auto-regressive model coefficients to identify structural damage (Sohn and Farrar 2001; Lei *et al.* 2003). In this study, these same system identification time-series models will be used to estimate the natural frequency and damping ratio associated with each mode of the dynamic system. By estimating modal stiffness and damping parameters, a damage detection methodology of enhanced sensitivity and one with stronger physical interpretation will result.

A mathematical description of an instrumented civil structure is needed to describe the system in both an undamaged and damaged structural state. Assuming the structural system to be linear and time-invariant, numerous system identification models can be calculated from digitized input-output data (Ljung 1999). From the available models, the autoregressive with exogenous input (ARX) time-series model is chosen because of its computational simplicity. For the IASC-ASCE benchmark structure, input excitations delivered by shakers and modal hammers are recorded thereby providing the complete input-output behavior of the system. Mathematically, an ARX model is a linear difference equation equating weighted past observations of the system output, $y(k)$, with those of the system input, $u(k)$:

$$y(k) + a_1 y(k-1) + \cdots a_{n_a} y(k-n_a) = b_1 u(k-1) + \cdots b_{n_b} u(k-n_b) + e(k) \tag{1}$$

The weights on past observations of the system output are denoted as a while those of the input are denoted as b. In total, n_a observations of the system output and n_b observations of the input are considered. The selection of the appropriate model size (n_a and n_b) is done using two separate sets of input-output response data. Using the first set, various ARX time-series models of different sizes are calculated and the model residual error, $e(k)$, measured for each. As the number of coefficients increase, the norm of the residual error vector, $\{e\}$, will exponentially reduced. The second set of input-output response data is then used as a validation data set. Using the calculated ARX models fit using the first data set, the model is used to predict the output response of the system, $y(k)$, using the second data set. As the model size increases, the residual error of the ARX model will reduce using the second data set. However, if the model size is made too large, the model will begin to over-fit the first data set thereby capturing noise processes hidden in the input-output data. At this point, the residual error of the ARX model using the second data set will begin to increase. The ARX model order is then selected before the point where the ARX error in predicting the second data set output stops decreasing and begins to increase.

Discrete-time signals, such as the recorded response of the structure, can be transformed to the complex-domain through the use of the *Z*-transform. The *Z*-transform is the discrete-time analog of the continuous-time Laplace transform. The *Z*-transform is used to transform the time-series model described by Equation (1) to the complex domain:

$$
\begin{aligned}
&Z\left\{y(k) + a_1 y(k-1) + \cdots a_{n_a} y(k-n_a) = b_1 u(k-1) + \cdots b_{n_b} u(k-n_b) + e(k)\right\} \Rightarrow \\
&\qquad Y(z) + a_1 z^{-1} Y(z) + \cdots a_{n_a} z^{-n_a} Y(z) = b_1 z^{-1} U(z) + \cdots b_{n_{ba}} z^{-n_b} U(z) + E(z)
\end{aligned}
\tag{2}
$$

Ignoring the residual error complex domain representation, *E(z)*, a transfer function of the dynamic linear system can be written in the discrete-time complex domain, *H(z)*:

$$
H(z) = \frac{Y(z)}{U(z)} = \frac{b_1 z^{-1} + \cdots b_{n_{ba}} z^{-n_b}}{1 + a_1 z^{-1} + \cdots a_{n_a} z^{-n_a}} \tag{3}
$$

The transfer function, *H(z)*, can be shown to be the Z-transform of the discrete-time response, *h(k)*, of the dynamic system to a unit-pulse input. The roots of the transfer function's polynomial denominator are termed the poles of the dynamic system because *H(z)* grows to infinity at the points. The number of poles in the ARX model discrete-time transfer function is equal to the number of ARX coefficients, n_a, on past observations of the system output. Representing the solution of the system characteristic equation, poles encapsulate the frequency, ω_n, and damping ratio, ξ, of each uncoupled response mode. To provide a visual aid of the frequency and damping associated with each mode of the system, the real-imaginary complex plane is often used for plotting pole locations. The reason for using the complex plan for this purpose is evident by examining the analytical relationship between frequency, damping ratio and pole location:

$$
z_{pole} = e^{-\xi\omega_n T} e^{\pm\omega_n\sqrt{1-\xi^2}\,jT} = re^{\pm j\theta} \tag{4}
$$

where the variable *T* is the discrete time step of the time sampled response data. The convenience of Equation (4) is that it describes pole location in polar coordinates with radius, *r*, and angle, θ. Using Equation (4), contours of constant frequency and damping ratio can also be superimposed on the complex plane to provide a visual reference of the frequency and damping associated with each pole location. Contours of constant frequency originate from the perimeter of the unit circle stability boundary. Similarly, contours of constant damping originate from *z=1+0j* and terminate along the real axis. By mapping contours of constant modal frequency and damping ratio, the complex plane is a powerful and highly expressive domain in which to analyze structural systems in their undamaged and damaged states. As damage is introduced in a structural system, subtle changes in the system stiffness and damping will occur, resulting in detectable migration of poles on the complex plane.

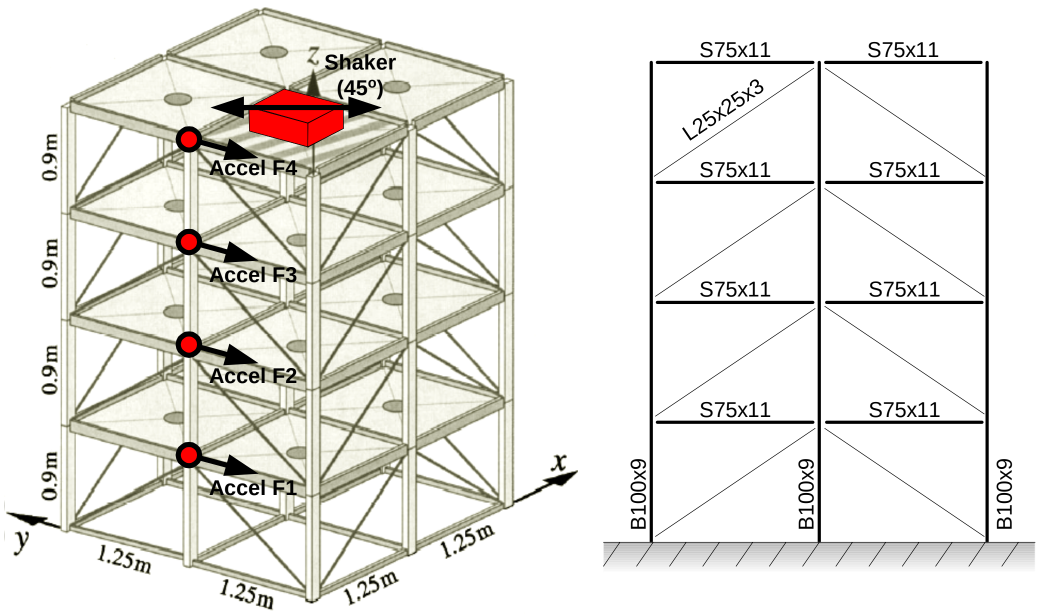

Figure 1. Illustration of the IASC-ASCE benchmark test structure with accelerometer and shaker locations labeled (adapted from Johnson *et al.* (2004)).

IASC-ASCE Benchmark Study Structure

Phase 2 of the IASC-ASCE structural health monitoring benchmark study consists of experimental testing of a large-scale laboratory steel structure in which damage is intentionally introduced. The steel structure is constructed using three steel sections for the columns (B100x9), beams (S75x11) and bracing elements (L25x25x3). As shown in Figure 1, the 4-bay structure consists of four floors, each 2.5 m by 2.5 in area, and stands 3.6 m tall. A variety of accelerometers are installed throughout the structure to record its response in the structure's weak (*y*, southward) and strong (*x*, westward) directions. Using the mounted accelerometers, the structure is monitored under ambient conditions as well as when vibrations are introduced using an electrodynamic shaker and modal hammer blows. In this study, only structural acceleration response data corresponding to random excitations generated using the electrodynamic shaker will be considered.

For excitation of the benchmark structure, a Ling Dynamic Systems V450 shaker is mounted to the top story of the test structure. With a total mass of 81.6 kg, the shaker is aligned such that the excitation direction is 45° relative to the both the strong and weak structural directions. An accelerometer is mounted to the shaker to records its acceleration during random white noise excitation of the structure. To record the response of the structure, accelerometers are mounted to the eastern face of the structure at each floor. With sensitivities of 5 V/g, the force balanced accelerometers are sufficiently accurate in recording the response of the structure during random excitations delivered by the shaker.

Table 1. Damaged configurations of the IASC-ASCE benchmark structure

Configuration	Description	# of Braces Removed
1	Undamaged - all braces installed	-
2	Eastside braces removed	8
3	Southeast bay braces removed	8
4	Only one southeast brace removed on 1^{st} and 4^{th} floors	2
5	All of the 1^{st} floor southeast bay braces removed	2

The structure is initially excited for 120 seconds using a random excitation record generated and applied by the shaker. This response of the structure corresponds to the structure in its undamaged state and is denoted as Configuration 1. As summarized in Table 1, an additional four configurations that represent the test structure in a damaged state (bracing members removed) are tested.

Damage Characterization of the IASC-ASCE Benchmark Structure

To first characterize the benchmark structure system using ARX time-series models, an appropriate model size (n_a and n_b) is sought. Using the aforementioned model order selection procedure, the ARX time-series model order is selected to be n_a = 16 and n_b = 2 using the two time-history data sets corresponding to the 4^{th} story response of the undamaged structure. The shaker mounted to the 4^{th} story is oriented 45° relative to the measured acceleration direction (southward). When calculating the different complex domain transfer functions between the shaker and each floor, $H_{i4}(z)$, the projection of the shaker force upon the measured acceleration direction is used. As shown in Figure 2, the ARX model determined for the undamaged structure predicts the system output with outstanding accuracy when compared to the true response measured at the 4^{th} story.

Each random excitation record applied by the shaker is 120 seconds long and the structural response is measured at a sample rate of 200 Hz. As a result, the 24000 point response record is delineated into eight separate records consisting of 3000 points each (15 seconds). By dividing the response of the structure in each structural configuration, a library of ARX models can be found for each structural state. This will permit tracking the location of ARX time-series model poles in the complex

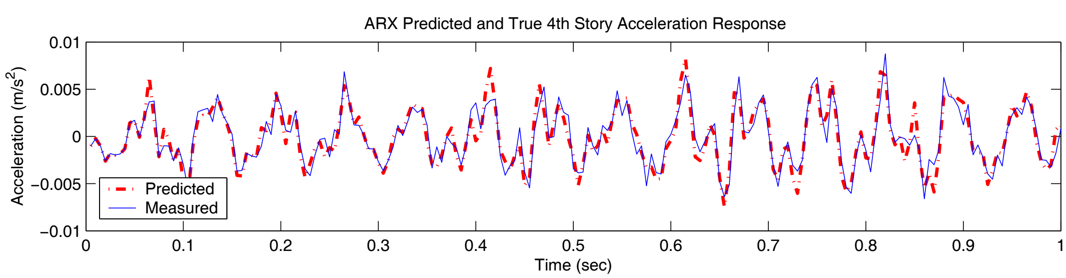

Figure 2. 4^{th} story response of the undamaged benchmark structure

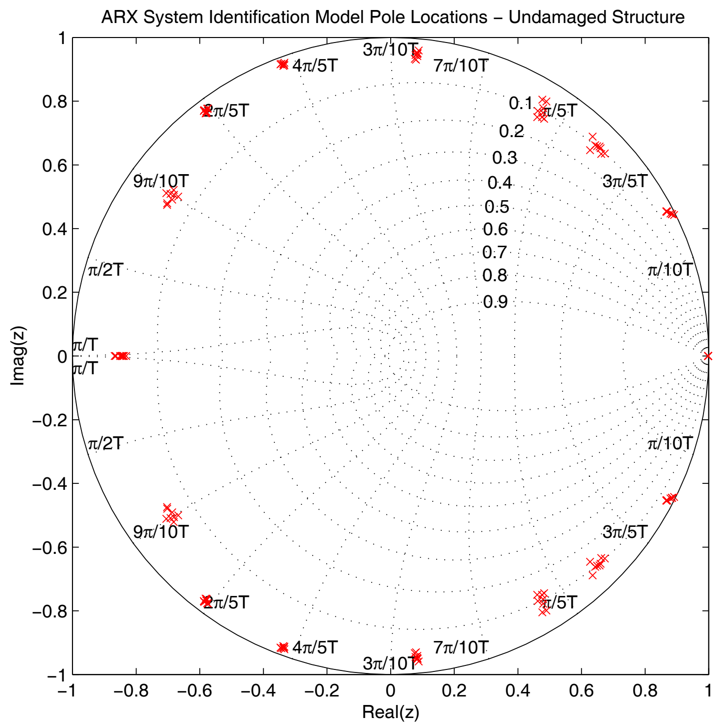

Figure 3. Pole location of the undamaged structure transfer function $H_{14}(z)$ (dotted lines represent contours of constant damping and frequency)

plane in a more rigorous manner because statistical methods can be used to define what constitutes a statistically significant migration. For example, using the input-output response measured at the 1st story, eight separate ARX models are calculated from the 120 second response record. The poles of the resulting ARX models, $H_{14}(z)$, are plotted upon the real-imaginary complex plane as shown in Figure 3. The well controlled behavior of the ARX model estimation should be noted as witnessed by the tight pole clusters formed for the eight individually calculated ARX models.

Eight ARX models are fit for each structural configuration (see Table 1) and each measured structure response. From the i^{th} degree-of-freedom measured, the poles of the complex-domain transfer function, $H_{i4}(z)$, are plotted upon the complex plane. As shown in Figure 4 for the 3rd story input-output acceleration response, the poles form seven complex conjugate pole clusters (as numbered) distributed at different frequencies. With eight models found for each structural configuration, the poles for each cluster are assumed to be distributed upon the complex plane by a Gaussian normal distribution whose mean and standard deviation can be estimated. Using a maximum-likelihood approach to finding the mean and standard deviation of each pole cluster, the first level curve of each cluster is superimposed upon the pole clusters depicted in Figure 4. The level curves are more legible in the four zoomed plots of the 2nd, 5th, 6th and 7th pole clusters presented to the right of the figure. The level curves serve to verify if the migration of pole clusters resulting from the different damage configurations are statistically significant. In this study, if the migration of the cluster mean is outside of the first level curve of the undamaged

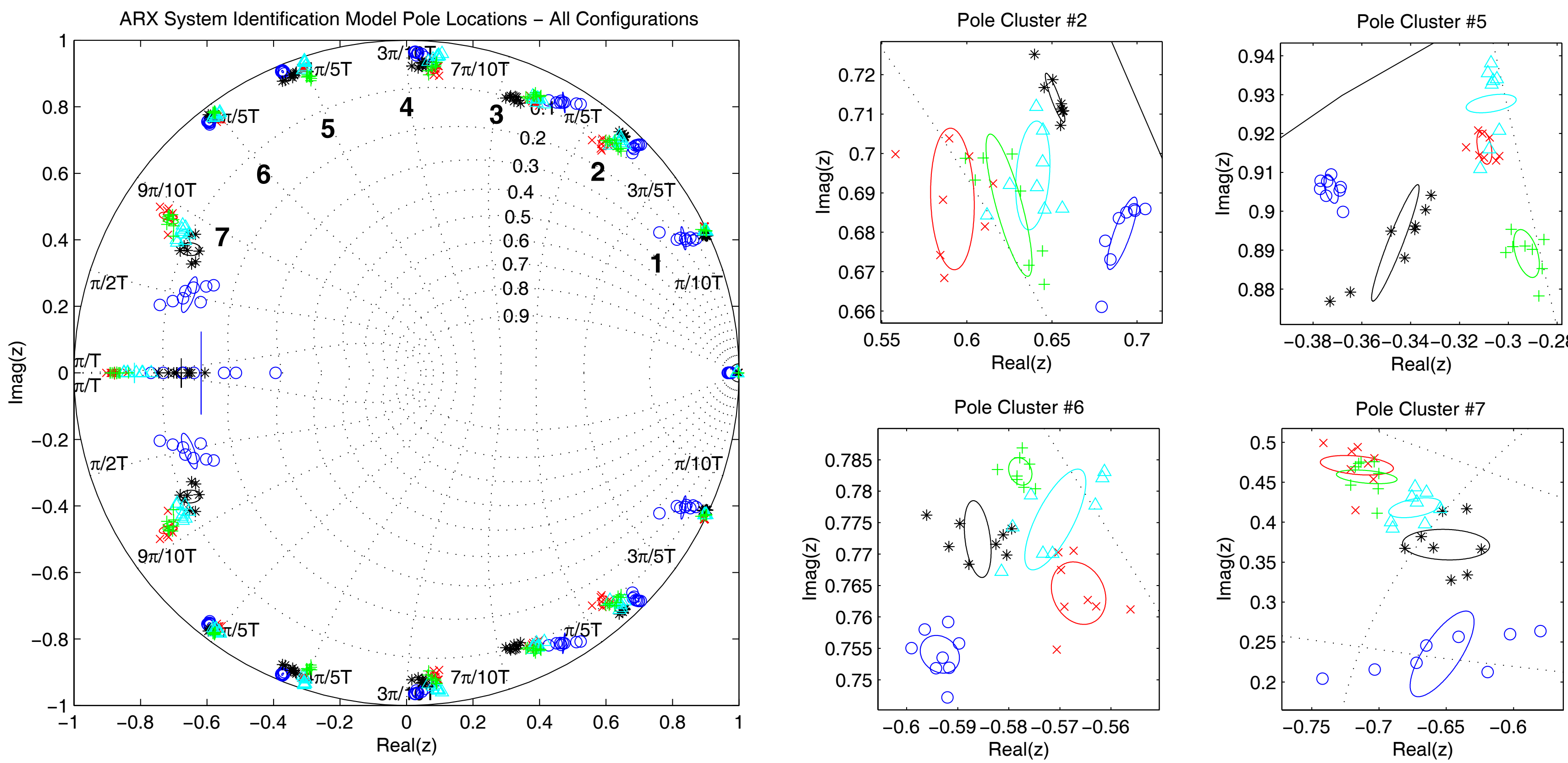

Figure 4. Pole locations of the transfer function *$H_{34}(z)$* for the undamaged and four damaged configurations (x = Configuration #1; o = Configuration #2; * = Configuration #3; ∇ = Configuration #4; + = Configuration #5)

(Configuration #1) benchmark structure clusters, then the migration is denoted as attributable to structural damage.

The pole clusters of the $H_{34}(z)$ complex-domain transfer function are plotted upon the same complex plane for all five structural configurations with the first level curve of each cluster superimposed. As the structural configuration is changed, there is a dramatic shift in the pole clusters as witnessed in Figure 4. While all of the clusters exhibit some migration, it is observed that pole clusters 2, 5, 6 and 7 exhibit the greatest sensitivity to the structural damage introduced in the structure. Figure 4 presents zoomed pictures of these clusters for all five structural configurations. For all four clusters, the migration of the cluster mean moves a significant amount with the introduction of damage in the system. With Configuration #2 representing the greatest amount of structural damage (all of the eastside braces removed), the pole clusters of this severely damaged configuration are situated far distances from the clusters of the undamaged structure. In a similar fashion, the clusters associated with Configuration #3 also experience dramatic migrations relative to the undamaged structure cluster locations upon the complex plane. For Configurations #4 and 5, a smaller amount of structural damage is introduced with only 2 braces removed for each configuration. As a result, the migration of the pole clusters can still be witnessed, but their migration is not of the same order as those for Configuration #2 and #3. Similar observations can be made from inspecting the pole plots corresponding to the ARX models calculated from the input-output response data measured at the other three model floors (1^{st}, 2^{nd}, and 4^{th} floors).

Conclusions

This study represents a novel approach to detecting damage for civil structures based on system identification models fit to input-output structural response data. Using the location of pole clusters upon the complex plane as the damage sensitive feature, all four damage scenarios tested upon the IASC-ASCE benchmark structure are easily identifiable. Furthermore, the degree of pole cluster migration appears to exhibit sensitivity to the extent of damage introduced (e.g. the number of braces removed) in the system. While the initial results presented in this paper suggest the method to be a powerful approach to damage detection, further work is needed to better understand how pole migrations are influenced by other factors such as structural environmental and operating conditions.

References

Doebling, S. W., Farrar, C. R., Prime, M. B. and Shevitz, D.W. (1996). *Damage identification and health monitoring of structural and mechanical systems from changes in their vibration characteristics: a literature review*. Technical Report No. LA-13070-MS, Los Alamos National Laboratory, Los Alamos, NM.

Johnson, E. A., Lam, H. F., Katafygiotis, L. S., and Beck, J. L. (2004), "Phase 1 IASC-ASCE structural health monitoring benchmark problem using simulated data," *Journal of Engineering Mechanics*, ASCE, 130(1), 3-15.

Lei, Y., Kiremidjian, A. S., Nair, K., Lynch, J. P. and Law, K. H. (2003), "An enhanced statistical damage detection algorithm using time series analysis," Proceedings of the 4th International Workshop on Structural Health Monitoring, Stanford, CA, September 15-17, 2003.

Ljung, L. (1999) *System Identification: Theory for the User*, Prentice Hall PTR, Upper Saddle River, NJ.

Lynch, J. P. (2004), "Linear classification of system poles for structural damage detection using piezoelectric active sensors," *Proceedings of the 11th Annual International Symposium on Smart Structures and Materials*, SPIE, San Diego, CA, March 14-18, 2004.

Park, G., Cudney, H. H., and Inman, D. J. (2000), "Impedance-based health monitoring of civil structural components," *Journal of Infrastructure Systems*, ASCE, 6(3), 153-160.

Sohn, H. and Farrar, C. (2001). "Damage diagnosis using time-series analysis of vibrating signals." *Journal of Smart Materials and Structures*, IOP, 10(3), 446-451.

Yuen, K. -V., Au, S. K. and Beck, J. L. (2004), "Two-stage structural health monitoring approach for phase 1 benchmark studies," *Journal of Engineering Mechanics*, ASCE, 130(1), 16-33.